Swelling Kinetics of Linseed Oil-Based Polymers

Vinay Sharma,[1,2] J. S. Banait,[2] P. P. Kundu[1]

[1]*Department of Chemical Technology, Sant Longowal Institute of Engineering and Technology, Sangrur, Punjab 148106, India*
[2]*Faculty of Physical Sciences, Punjabi University, Patiala, Punjab 147002, India*

Received 28 January 2008; accepted 1 July 2008
DOI 10.1002/app.29006
Published online 4 November 2008 in Wiley InterScience (www.interscience.wiley.com).

ABSTRACT: Kinetics of swelling and sorption behavior of copolymers (based on linseed oil, styrene, divinylbenzene, and acrylic acid via cationic and thermal polymerization) is studied in tetrahydrofuran (THF) at different temperatures. The values of n in the transport equation are found to be below 0.4, showing non-Fickian or pseudo-Fickian transport in the polymers. The dependence of diffusion coefficient on the composition and temperature has also been studied for the linseed oil-based polymers. The diffusion coefficient in cationic samples decreases with an increase in the oil contents in the samples. In case of thermal samples, the diffusion coefficient first increases up to 30% oil contents and then decreases. The diffusion coefficient decreases with an increase in temperature for all of the linseed oil polymer samples. The sorption coefficient increases with an increase in the oil contents for all samples. The crosslink density (calculated from the THF swelling) ranges from 20.16 to 92.34 $\times$ 10^6 mol/cm^3 for cationic samples and 20.62 to 86.01 $\times$ 10^6 mol/cm^3 for thermal samples.
 J Appl Polym Sci 111: 1816–1827, 2009

Key words: linseed oil polymers; diffusion; sorption; swelling kinetics; crosslink density; pseudo-Fickian diffusion

INTRODUCTION

Sorption and diffusion of the solvents in and through polymers have been widely investigated from both theoretical as well as experimental point of view.[1–3] The swelling technique is a commonly used method to determine various coefficients such as diffusion, sorption, and permeability coefficient.[4–8] In swelling experiments, the polymer of known dimension is dispersed in a solvent, and the solvent mass uptake versus time is recorded and the data is used to calculate the various coefficients. These coefficients give an idea about the use of polymers in various applications such as membranes, ion-exchangers, controlled release systems, packaging, microchip manufacturing, etc.

Sorption kinetics in polymers exhibits a variety of deviations from normal Fickian behavior, attributable to (a) slow viscous relaxations of the swelling polymer or (b) differential swelling stresses generated by the constraints imposed on local swelling during sorption. Several models have been proposed for the study of the swelling behavior of the polymers.[9–11] *In situ* study by FTIR-ATR is also carried out by many researchers for the prediction of the sorption behavior of the polymers.[12–14]

Linseed oil is a triglyceride of linolenic acid (53%), oleic acid (18%), linoleic acid (15%), palmitic acid (6%), and stearic acid (6%).[15] Linseed oil is considered as a good drying oil, which is mainly used for the preparation of paints and varnishes.[16] It is also used in enamels, linoleum, oilcloth, patent leather, printer's ink, and as waterproofing for raincoats, slickers, and tarpaulins.[17] Considerable research has been carried out on applications of linseed oil. In medicinal front, it is claimed that linseed oil is useful in treating anxiety, prostate problems, vaginitis, weight loss, and certain types of cancer,[18] but appropriate research is lacking. To improve its film properties, different olefinic monomers, such as styrene, have been copolymerized with linseed oil.[19–21] Recently, it has been reported[22] that the reaction of styrene with drying oils depends on the number of conjugated double bonds present in the drying oil.

In this study, a new system of linseed oil-based polymers (see structure in Scheme 1) is studied for sorption kinetics in tetrahydrofuran (THF). The variation in sorption is studied with respect to temperature. The rationale of this work is to study the cationic and thermal polymers from linseed oil with an alteration in the oil contents. The mechanism of the sorption is studied from the data by a linear fit of the equation of the transport phenomena.

Correspondence to: P. P. Kundu (ppk923@yahoo.com).

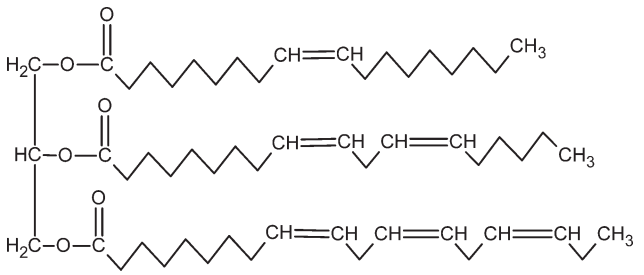

Scheme 1 Structure of linseed oil.

EXPERIMENTAL

Materials

Common linseed oil of commercial grade is procured from local market, and conjugated linseed oil (87% conjugation) is purchased from Alnor Oil Company Alnor, NY. Styrene, acrylic acid, THF, and boron trifluoride diethyl etherate complex are purchased from Merck Chemical, Germany. Divinylbenzene (DVB) is purchased from Fluka Chemie. Dicyclopentadiene (DCP) is purchased from Himedia Laboratories Pvt., Mumbai (India).

Sample preparation

Cationic sample preparation

Polymeric materials have been prepared by heating desired concentrations of common linseed oil, styrene, and DVB in glass molds. The desired amount of styrene and DVB is added to the linseed oil and the mixture is vigorously stirred. Then, the mixture is cooled and the initiator is added with constant stirring at low temperature, and the whole mass is transferred to the glass mold. The sealed glass mold is kept at room temperature for 12 h and then heated sequentially at different temperatures, such as 12 h at 60°C, 24 h at 110°C, and finally postcured at 120°C for 3 h. The nomenclature used in this work is based on the original composition of reactants (shown in Table I). For example, Lin30 represents a sample containing 30% linseed oil, 46.5% styrene, 15.5% DVB, and 8% initiator.

Thermal sample preparation

Polymeric materials have been prepared by heating desired concentrations of conjugated linseed oil, acrylic acid, and DVB in glass vials. The desired amount of acrylic acid and DVB is added to the conjugated linseed oil and the mixture is vigorously stirred. The glass vial is heated sequentially at different temperatures, such as 6 h at 80°C, 12 h at 100°C, 12 h at 120°C, and finally postcured at 140°C for 12 h. The nomenclature used in this work is based on the original composition of reactants (shown in Table I). For example, CLin0 represents a sample containing 0% linseed oil, 90% acrylic acid, and 10% DVB.

Swelling experiments

The samples are cut into circular form using a die of 10 mm diameter and 15 mm thickness. The thickness of the samples is measured by means of a screw gauge. The dry samples are weighed on an electronic balance (Citizen, CX 220) and then kept in the solvent in screwed bottles. The samples are taken out of the solvent at specific intervals and the excess solvent is rubbed off. The samples are then weighed and again immersed in the solvent till equilibrium is attained (i.e., 72 h). The time for measuring weight of the sample is kept minimal (about 30 s), so that the escape of the solvent from the sample remains negligible. Equilibrium swelling experiments at different temperature are carried out at 25, 30, 35, and

TABLE I
Detailed Composition of the Polymer Samples Prepared From Linseed Oil

Sample ID[a]	Linseed oil (%)	Styrene (%)	Divinylbenzene (%)	Acrylic acid (%)	Initiator (%)	Dicyclopentadiene (%)
Lin30	30	46.5	15.5	–	8	–
Lin40	40	39	13	–	8	–
Lin50	50	31.5	10.5	–	8	–
Lin60	60	24	8	–	8	–
DCP5	50	32	5	–	8	5
DCP7	40	38	7	–	8	7
DCP16	60	–	16	–	8	16
CLin0	0	–	10	90	–	–
Clin10	10	–	10	80	–	–
CLin20	20	–	10	70	–	–
CLin30	30	–	10	60	–	–
CLin40	40	–	10	50	–	–
CLin50	50	–	10	40	–	–
CLin60	60	–	10	30	–	–

[a] CLin samples contain 87% conjugated linseed oil.

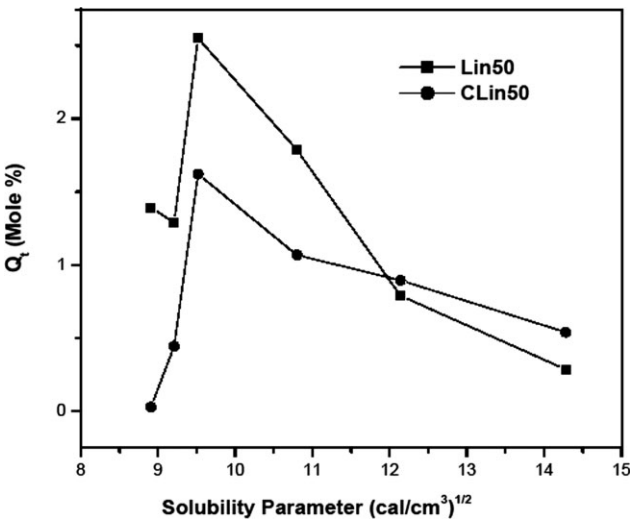

Figure 1 Plot of volume equilibrium of swelling (Q) versus solubility parameter (δ) for Lin50 and CLin50 samples. The δ values in (cal/cm^3)$^{1/2}$ of the used solvents are 8.91 (toluene), 9.21 (chloroform), 9.52 (THF), 10.8 (dimethyl acetamide), 12.14 (dimethyl formamide), and 14.28 (methanol).

40°C (±1°C) to study the effect of temperature on the swelling. For the temperatures higher than room temperature, the samples are kept in a microprocessor-controlled hot air oven.

The mole percent uptake (Q_t) at each time interval is calculated by using eq. (1).[23]

$$Q_t = \frac{M_e}{M_r} \times \frac{100}{M_i} \quad (1)$$

where M_e is the mass of the solvent taken up at equilibrium, M_r is the relative molecular mass of the solvent, and M_i is the mass of the dry sample. The mole percent uptake at 72 h is taken as swelling at infinite time (Q_∞).

Equilibrium swelling experiments are also performed at 25°C ± 1°C to determine the solubility parameter of the samples, prepared by cationic and thermal polymerization. The swelling is carried out in various solvents of solubility parameters ranging from 8.91 to 14.51 (cal/m^3)$^{1/2}$. From the plots of equilibrium swelling volume (Q_t) versus the solubility parameter (δ), THF gives the maximum value of Q in all the samples, and hence is used for further kinetic studies. Figure 1 shows the representative plot of volume equilibrium swelling versus solubility parameter for Lin50 and CLin 50 samples.

Optical characterization of swelled samples

The samples are monitored through an optical microscope (Digital Blue-QX5, PC controlled). The swelled samples are observed through optical microscope, and photographs are taken at different magnifications.

RESULTS AND DISCUSSION

Swelling of polymer samples

The mole percent uptake of the solvent is plotted against square root of time. The plots for the mole percent uptake are shown in Figures 2 and 3 for cationic and thermal samples at a temperature of 25°C ± 1°C. In Figure 2, it is observed that the swelling of the samples increases with an increase in the oil contents. The sample containing 30% linseed oil shows a minimum swelling, whereas the sample with 60% linseed oil contents shows a maximum swelling. This can be explained by a decrease in the rigid part or crosslinker with an increase in the linseed oil contents, resulting in more flexible and rubbery polymeric chains. In addition to DVB, when DCP is added in the mixture, the resulting polymer shows a decrease in the swelling. In DCP system, the sample with 5% DCP contents shows a maximum, and the sample with 16% DCP contents shows a minimum swelling, i.e., with increasing DCP contents, the swelling decreases. The content of crosslinkers (DVB and DCP) is the lowest (10%) and the highest (32%) in the DCP5 and DCP16 sample, respectively (see Table I). This results in a decrease and an increase in crosslink density in DCP5 and DCP16 samples, respectively. Therefore, DCP16 shows a minimum and DCP5 shows a maximum swelling.

Figure 3 shows the mole percent uptake of solvent for the thermal samples. In these samples, the CLin0 sample shows a minimum and CLin60 shows a maximum swelling. The reason for change in solvent

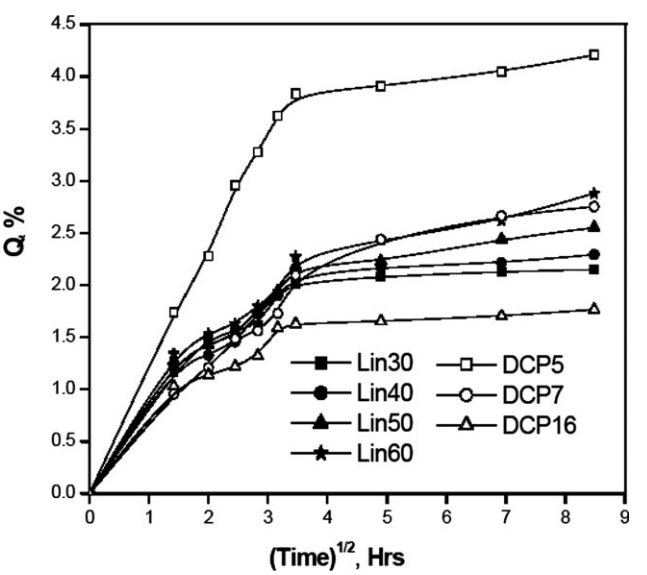

Figure 2 Sorption curve showing mole percent uptake of cationic samples with different compositions at 25°C.

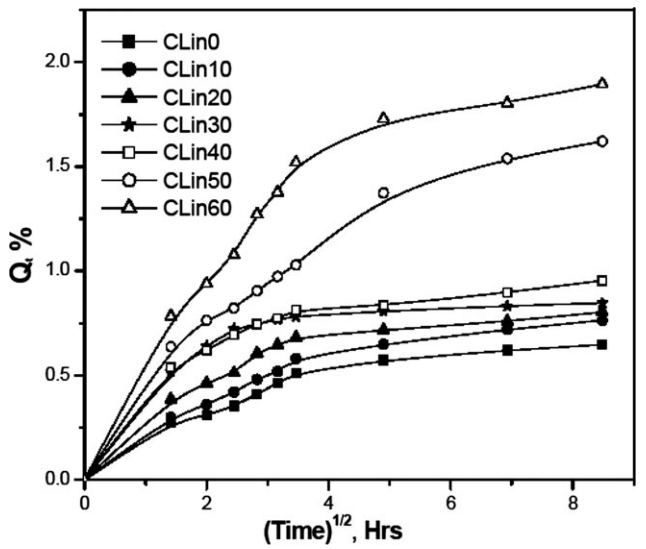

Figure 3 Sorption curve showing mole percent uptake of thermal samples with different compositions at 25°C.

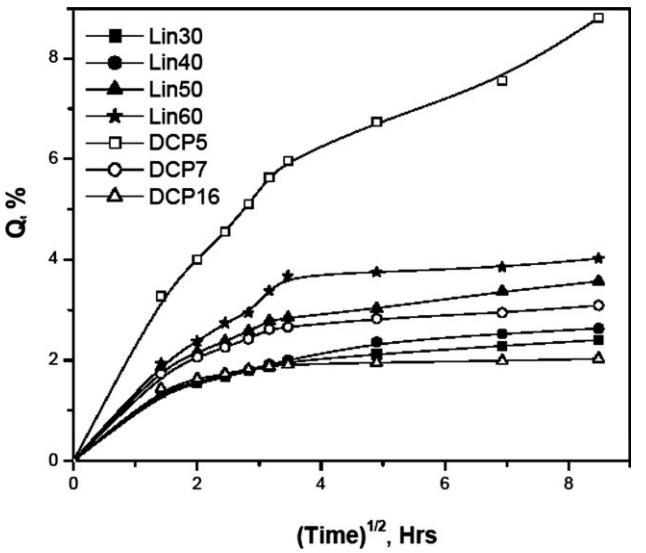

Figure 4 Sorption curve showing mole percent uptake of cationic samples with different compositions at 30°C.

uptake is the alteration in composition of the polymer sample (for composition see Table I). In CLin0 sample, conjugated linseed oil contents are nil, and in CLin60 sample, it is 60%. Thus, on proceeding from CLin 0 to Clin 60 sample in the table, the oil moieties in the sample increases and the rigid part of the sample decreases. When the samples from both procedures (thermal and cationic) are compared, the thermal samples show a minimum swelling. This is due to the reason that in thermal polymerization 87% conjugated linseed oil is used. This is more reactive due to presence of conjugation, and hence resulted in highly crosslinked polymers.

Figures 4–9 show the sorption curves for the cationic and thermal samples at different temperatures. It is clear from the Figures 2–9 that with an increase in temperature from 25 to 40°C, the swelling rate is also increased. In the swelling of cationic samples, a two stage sorption is evident in almost all of the samples, except of DCP5. It is due to a quasi-equilibrium, which first reached rapidly at the polymer surface and then by simple diffusion throughout the polymer sample.[24] The second stage of sorption is associated with an increase in surface concentration, which occurs slowly compared to the diffusion process and is the rate-determining factor for sorption. The concentration is virtually uniform throughout the sheet and increases at a rate, independent of the thickness. In thermal samples, at first, the rate of uptake increases as sorption proceeds, but later decreases as the final equilibrium is approached. These curves are often referred to as sigmoid sorption curves.[25] They are generated because of the reason that the surface equilibrium conditions are not established instantaneously.

Figure 4 shows the sorption curves as the mole percent uptake versus square root of time for cationic samples at 30°C. The swelling for the samples is almost double than swelling for the samples at 25°C. The sorption curves at higher temperatures (Figs. 6 and 7) show a modest increase in swelling. It is observed that with an increase in the temperature, the solvent penetration increases, resulting in higher swelling of the polymer. The sorption curves for all the samples are almost asymptotic with very little increase in the swelling after 12 h except for DCP5, which shows a plateau after 72 h. Figure 6 shows the sorption curves as mole percent uptakes of solvent versus square root of time at 35°C. All the

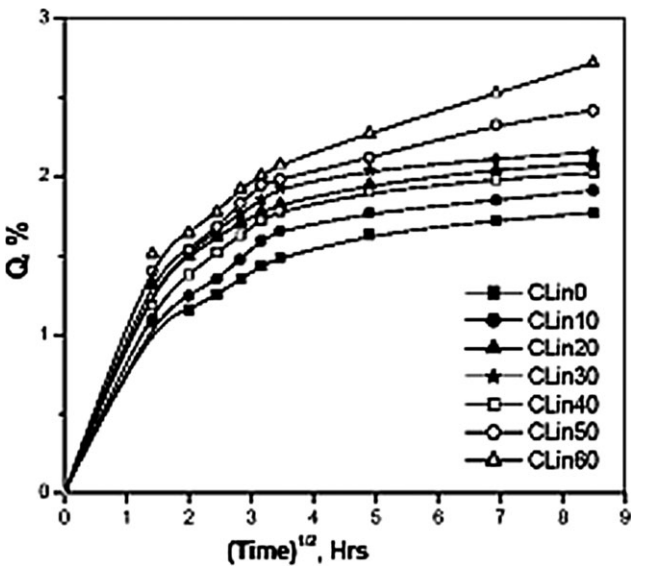

Figure 5 Sorption curve showing mole percent uptake of thermal samples with different compositions at 30°C.

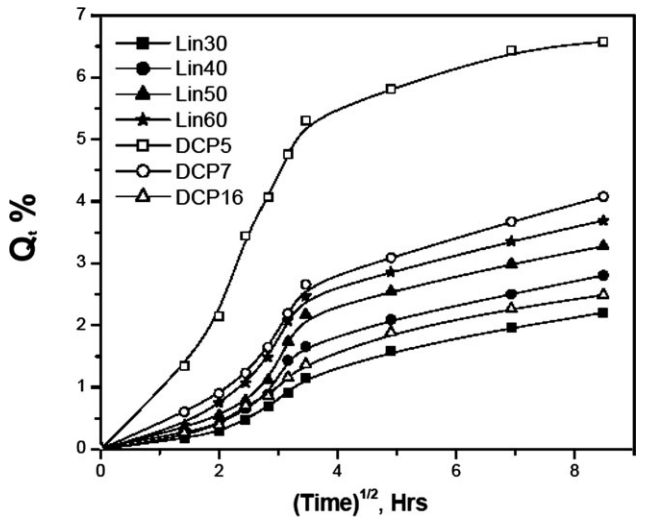

Figure 6 Sorption curve showing mole percent uptake of cationic samples with different compositions at 35°C.

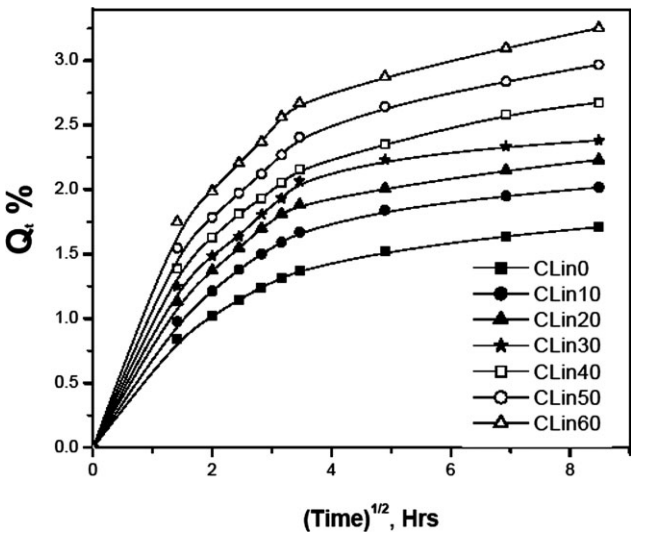

Figure 7 Sorption curve showing mole percent uptake of thermal samples with different compositions at 35°C.

sorption curves show rapid growth up to first 6 h, then slight decrease or holdup, and then again sorption increases up to 12 h. After 12 h, all the curves become nearly parallel except for DCP5, which still shows an increase in the sorption up to 48 h. These curves are the typical examples of two stage sorption.[24] Figure 8 shows the sorption curves for the samples at 40°C. The DCP16 sample shows a minimum sorption and DCP5 shows a maximum sorption. Initially, DCP16, Lin30, and Lin40 show similar sorption up to 10 h, and after that there is a slight increase in the sorption of Lin30 and Lin40 samples. All the samples show an increase in the solvent uptake up to 12 h, and then the curves becomes almost parallel to the time axis except for DCP5, which shows an increase in the sorption up to 72 h. DCP is less reactive than DVB, when it is at 5% level; the resulting polymer is less crosslinked. Because of this, the polymer chains relax easily and the curve shows continuous increase in sorption for DCP5 sample.

The swelling of the thermal samples is presented in Figures 3, 5, 7, and 9 at 25, 30, 35, and 40°C, respectively. It is observed that the swelling increases almost twofold on increasing the temperature from 25 to 30°C (Figs. 3–5). On increasing the temperature from 30 to 40°C (Figs. 5,7, and 9), a modest increase in swelling is observed. In the thermal samples, a uniform increase in the swelling with increasing oil content is observed. Figure 5 shows a rapid increase in the sorption rate for all samples up to 12 h and then the sorption curves become almost parallel to the *x*-axis. On comparing the samples with different oil contents, the sample with minimum oil content (CLin0) shows a minimum, and the sample with maximum oil content (CLin60) shows a maximum swelling at any instance during swelling. The swelling ratio increases uniformly in all the samples. These curves are the fine example of the sigmoidal sorption curves.[25] Linseed oil is known for its plasticization effect in polymers.[26–28] It is apparent from the sorption behavior of the samples that the pendent linseed moieties present in the linseed-based polymers have a plasticization effect. When a small proportion of linseed oil is present in the polymer composition, the resulting polymers of linseed oil become rigid. The increased rigidity causes an increase in the resistance to the solvent. When the content of linseed oil is increased in the composition, the polymer chain relaxes easily and

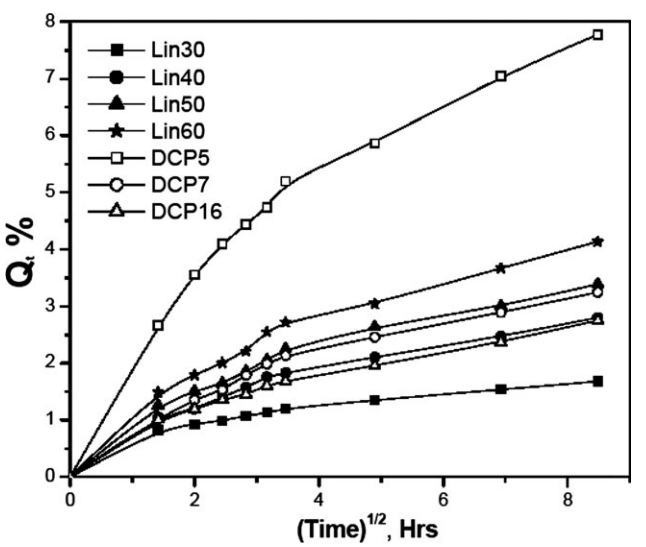

Figure 8 Sorption curve showing mole percent uptake of cationic samples with different compositions at 40°C.

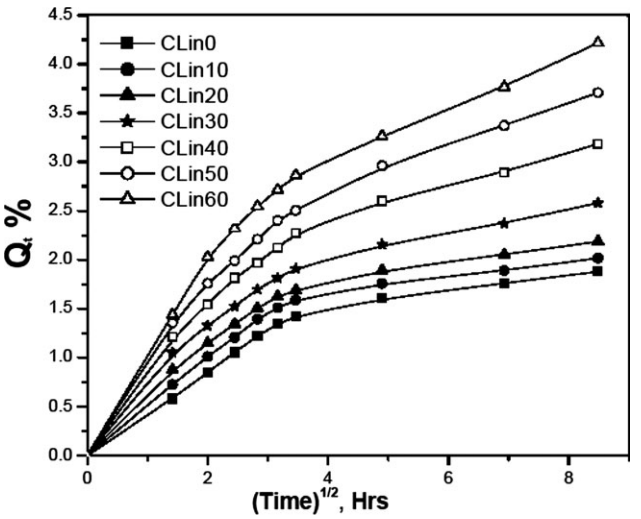

Figure 9 Sorption curve showing mole percent uptake of thermal samples with different compositions at 40°C.

arranges itself to adjust the incorporation of the small solvent molecules.

To find out the mechanism of swelling, the diffusion data is fitted into an empirical equation [eq. (3)][29] derived from the equation of transport phenomena [eq. (2)][23]

$$\frac{Q_t}{Q_\infty} = kt^n \tag{2}$$

$$\ln\frac{Q_t}{Q_\infty} = \ln k + n\ln t \tag{3}$$

where Q_t and Q_∞ are the mole percent uptake of solvent at time t and at infinity or equilibrium. k is a constant, which depends upon the solvent-polymer interaction and the structure of the polymer. For all the samples, the regression coefficient (r) varies between 0.88 and 0.99. The values of constant k and n obtained from the eq. (3) and Q_∞ are reported in Tables II and III. The value of n gives an idea of the mechanism of sorption.[30] For the value of n of 0.5, the mechanism of swelling is termed as Fickian transport. This occurs, when the rate of diffusion of solvent is smaller than polymer segmental mobility. If the value of n is not 0.5, then the transport is considered as non-Fickian. In particular, if $n = 1$, the transport is called "case II" transport.[30] It is a special case, where the solvent front moves with constant velocity. If n lies between 0.5 and 1, then it is called anomalous transport.[30] For non-Fickian transport, diffusion is more rapid than the polymer relaxation rate. For anomalous transport, the diffusion and relaxation rates are comparable.[30] If sorption is less

TABLE II
Values of Mole Percent Uptake at Infinite Time (Q_∞), n, k, and Standard Deviation (SD) for Cationic Samples at Different Temperatures

Temperature (°C)	Sample ID	Q_∞ (mol %)	n	k	SD
25	Lin30	2.149	0.165	0.159	0.092
	Lin40	2.293	0.190	0.109	0.096
	Lin50	2.551	0.205	0.125	0.076
	Lin60	2.881	0.221	0.147	0.058
	DCP5	4.209	0.229	0.603	0.149
	DCP7	2.753	0.307	−0.178	0.092
	DCP16	1.765	0.158	−0.032	0.086
30	Lin30	2.567	0.181	0.19	0.023
	Lin40	2.899	0.208	0.169	0.016
	Lin50	3.566	0.196	0.467	0.052
	Lin60	4.021	0.199	0.645	0.104
	DCP5	8.811	0.281	0.995	0.072
	DCP7	3.09	0.159	0.516	0.078
	DCP16	2.032	0.088	0.377	0.048
35	Lin30	2.084	0.377	−1.83	0.336
	Lin40	2.390	0.378	−1.691	0.314
	Lin50	3.364	0.306	−1.607	0.311
	Lin60	3.542	0.343	−1.143	0.326
	DCP5	7.764	0.278	−0.193	0.309
	DCP7	2.832	0.383	−1.414	0.44
	DCP16	1.630	0.461	−2.266	0.526
40	Lin30	1.474	0.202	−0.344	0.016
	Lin40	2.799	0.277	−0.137	0.044
	Lin50	3.072	0.282	0.041	0.041
	Lin60	4.345	0.286	0.214	0.043
	DCP5	9.647	0.286	0.868	0.049
	DCP7	2.912	0.315	−0.115	0.063
	DCP16	2.155	0.277	−0.19	0.02

TABLE III
Values of Mole Percent Uptake at Infinite Time (Q_∞), n, k, and Standard Deviation (SD) for Thermal Samples at Different Temperatures

Temperature (°C)	Sample ID	Q_∞ (mol %)	n	k	SD
25	CLin0	0.647	0.258	−1.445	0.085
	CLin10	0.764	0.286	−1.405	0.088
	CLin20	0.803	0.201	−0.998	0.087
	CLin30	0.846	0.119	−0.602	0.077
	CLin40	0.954	0.151	−0.653	0.053
	CLin50	1.621	0.278	−0.658	0.043
	CLin60	1.895	0.275	−0.425	0.123
30	CLin0	1.771	0.148	−0.016	0.036
	CLin10	1.912	0.156	0.043	0.055
	CLin20	2.114	0.127	0.244	0.04
	CLin30	2.127	0.133	0.261	0.053
	CLin40	2.229	0.146	0.148	0.058
	CLin50	2.417	0.155	0.256	0.037
	CLin60	2.718	0.166	0.293	0.018
35	CLin0	1.906	0.193	−0.224	0.055
	CLin10	2.006	0.195	−0.05	0.071
	CLin20	2.204	0.182	0.096	0.07
	CLin30	2.340	0.18	0.181	0.069
	CLin40	2.736	0.182	0.228	0.043
	CLin50	2.985	0.184	0.354	0.045
	CLin60	3.288	0.174	0.483	0.046
40	CLin0	1.825	0.307	−0.546	0.133
	CLin10	1.946	0.267	−0.322	0.117
	CLin20	2.186	0.243	−0.168	0.088
	CLin30	2.405	0.241	−0.022	0.063
	CLin40	3.043	0.261	0.1	0.06
	CLin50	3.935	0.273	0.193	0.049
	CLin60	4.374	0.277	0.305	0.07

than 0.5, then it is termed as pseudo-Fickian transport. It is characterized by initial curvature of the Q_t versus $t^{1/2}$ plots out of the origin concave to the time axis.[31,32] From Tables II and III, the values of n fall below 0.4, indicating the transport as pseudo-Fickian.

The swelling data is used to calculate diffusion coefficient (D), which is a measure of the ability of the solvent molecules to move among the polymer and the sorption coefficient (S), which gives an idea about the equilibrium sorption. The diffusion coefficient (D) is calculated as[33]

$$D = \pi\left(\frac{h\theta}{4Q_\infty}\right)^2 \tag{4}$$

where $\pi = 3.14$; h is the thickness of the dry sample and θ is the slope of the initial linear portion of the curve Q_t versus $\sqrt{t}$; and Q_∞ is the mole percent uptake of the solvent at infinite time.

The sorption coefficient (S) is calculated as[33]

$$S = \frac{M_\infty}{M_p} \tag{5}$$

where M_∞ is the mass of the solvent uptake at equilibrium and M_p is the mass of the dry sample. The sorption and diffusion coefficients are used to calculate permeability coefficient (P) of the samples, which is given by[33]

$$P = D \times S \tag{6}$$

The values of these coefficients are reported in Tables IV and V. It is observed that for cationic samples, DCP16 sample shows the highest and the Lin60 sample shows the lowest diffusion coefficient. The diffusion coefficient of the cationic samples decreases with an increase in the oil contents from 30 to 60% (Table IV). This may be due to the increase in the oily part, which relaxes easily and thus providing space to the solvent and increasing the diffusion of solvent in the polymer network. Also, the amount of crosslinker decreases with an increase in the linseed oil contents, which give rise to the looser structures with higher swelling capacity. The diffusion coefficient decreases with an increase in the temperature for all cationic samples. The decrease in the diffusion coefficient is due to the dominance of the oily portion in the polymer matrix. When DCP is added to the system, just opposite behavior is observed. The sample with 40% linseed oil shows a minimum, whereas the sample with 60% oil shows a maximum diffusion coefficient. This may be attributed to the presence of DCP and DVB,

TABLE IV
Diffusion Coefficient (*D*), Sorption Coefficient (*S*), and Permeability Coefficient (*P*) in THF for Cationic Samples at Different Temperatures

Temperature (°C)	Sample ID	$D \times 10^4$ (cm^2/s)	S (g/g)	$P \times 10^4$ (cm^2/s)
25	Lin30	4.39	1.55	6.81
	Lin40	3.99	1.65	6.58
	Lin50	3.38	1.84	6.22
	Lin60	2.73	2.07	5.65
	DCP5	3.17	3.03	9.61
	DCP7	2.74	1.98	5.43
	DCP16	5.82	1.27	7.39
30	Lin30	3.38	1.13	3.82
	Lin40	2.86	1.37	3.92
	Lin50	2.82	1.85	5.22
	Lin60	3.08	2.18	6.71
	DCP5	1.09	6.34	6.91
	DCP7	1.09	2.22	2.42
	DCP16	5.08	1.46	7.42
35	Lin30	2.09	1.50	3.14
	Lin40	1.61	1.72	2.77
	Lin50	1.57	2.42	3.80
	Lin60	2.17	2.55	5.53
	DCP5	1.72	5.59	9.62
	DCP7	1.58	2.04	3.22
	DCP16	2.00	1.17	2.34
40	Lin30	2.78	1.06	2.95
	Lin40	2.29	2.02	4.63
	Lin50	2.10	2.21	4.64
	Lin60	1.93	3.13	6.04
	DCP5	1.23	5.95	7.32
	DCP7	2.24	2.10	4.70
	DCP16	2.63	1.24	3.26

which increases the crosslinking of the polymer. For a solvent, it is difficult to diffuse in the highly crosslinked polymer network.

The thermal polymeric systems show an initial increase in the diffusion coefficient, followed by a decrease with an increase in the oil content (Table V). The samples with an increase in oil contents (from 0 to 30%) show an increase in the diffusion coefficient, followed by a subsequent decrease on increasing oil content up to 60%. For the low oil contents (0 to 30%) in the polymer samples, the diffusion coefficient is high and as the oil contents increases from 30% onward, the diffusion coefficient starts decreasing. With an increase in the temperature, the diffusion coefficient decreases. At 35 and 40°C, the polymers with 0–20% oil contents show an increase in diffusion coefficients and then the diffusion coefficient decreases with an increase in the oil content.

The diffusion coefficient decreases with an increase in the temperature for both cationic and thermal samples. This is due to the increase in the relaxation in the polymer chain segments, which results in the increase in the entrapment of the solvent molecules in the vacant spaces (or holes). This results in a decrease in the diffusion of the solvent through the polymer matrix.

In case of sorption (Tables IV and V), the coefficient increases with an increase in the oil contents in the polymer matrix, but it decreases with an increase in the temperature. It may be attributed to the segmental motion of the bulky oil portion in the polymer, which adjusts to the penetrant molecules. In DCP samples, sorption coefficient decreases with an increase in the DVB and DCP contents. This is due to the higher crosslinker contents, which results in the more crosslinked structure. For the thermal samples, the sorption coefficient at 25°C decreases with increasing oil contents. The sorption coefficient starts increasing with an increase in the oil contents at higher temperatures.

In all the systems, it is observed that the sorption and diffusion coefficients decrease with an increase in the temperature. It is reported elsewhere [29,34] for natural and styrene–butadiene rubber that these coefficients show an increase with the rise in temperature. But in our case, these coefficient decreases with temperature. This can be explained by the dual mode model for diffusion in the polymers below glass transition temperature.[35–39] According to this

TABLE V
Diffusion Coefficient (*D*), Sorption Coefficient (*S*), and Permeability Coefficient (*P*) in THF for Thermal Samples at Different Temperatures

Temperature (°C)	Sample ID	$D \times 10^5$ (cm^2/s)	S (g/g)	$P \times 10^5$ (cm^2/s)
25	CLin0	2.98	0.78	2.32
	CLin10	2.81	0.73	2.05
	CLin20	3.62	0.67	2.45
	CLin30	4.33	0.61	2.64
	CLin40	3.50	0.47	1.65
	CLin50	1.89	0.45	0.85
	CLin60	0.92	0.44	0.40
30	CLin0	1.87	1.28	2.40
	CLin10	2.14	1.38	2.96
	CLin20	2.04	1.52	3.10
	CLin30	2.21	1.53	3.37
	CLin40	2.22	1.61	3.57
	CLin50	1.87	1.74	3.25
	CLin60	1.54	1.96	3.03
35	CLin0	3.01	1.37	4.12
	CLin10	3.10	1.44	4.46
	CLin20	3.12	1.66	5.17
	CLin30	3.08	1.68	5.17
	CLin40	2.63	1.97	5.18
	CLin50	2.51	2.15	5.39
	CLin60	2.47	2.37	5.85
40	CLin0	2.91	1.31	3.81
	CLin10	3.02	1.40	4.23
	CLin20	2.80	1.57	4.40
	CLin30	2.42	1.73	4.18
	CLin40	2.09	2.19	4.57
	CLin50	1.82	2.83	5.15
	CLin60	1.74	3.15	5.48

model, glassy polymers contain a distribution of microvoids frozen into the structure as the polymer is cooled through its glass transition temperature. The free segmental rotations of the polymer chains in the glassy state are restricted, which results in the fixed microvoids throughout the polymer. These microvoids in the glassy polymer network immobilize the solvent molecules by entrapment. The entrapments increase the size of the polymer, resulting in the enlargement of the microvoids. The enlarged microvoids further leads to initiate the macrofractures in the polymer (see Fig. 12). Diffusion and permeability are considered to be activated by temperature, so diffusion and permeability should increase in our case also. The decrease can only be ascribed to the dual mode sorption due to which the solvent molecules block the holes or microvoids, resulting in a decrease in diffusion of the solvent through the polymer matrix. Hu and Chou worked on swelling and development of porous structure in the ionic poly(acrylonitile-acrylamide-acrylic acid) hydrogels.[40] They suggested that the solvent diffusion involves the traveling through the pores in a restricted manner. Therefore, increase in temperature can lead to the increase in the void size and results in decrease in diffusion coefficient with temperature.

The permeability coefficients of the samples are the product of the diffusion and sorption coefficients. The permeability coefficients in cationic and thermal samples show an increase with increasing contents of linseed oil. It is observed that the DCP system has the highest values of the permeability coefficients, showing the high permeability of the DCP system.

Crosslink density and molecular weight

The sorption data are also used to calculate the crosslink density of the polymer networks using Flory-Rehner's equation[41]

$$\nu = -\frac{\ln(1 - V_p) + V_p + \chi V_p^2}{V_1(V_p^{1/3} - 0.5V_p)} \tag{7}$$

where V_p is the volume fraction of the polymer in the mixture, χ is the polymer-solvent interaction parameter, and V_1 is the molar volume of the solvent. V_p and χ are obtained by the following equations[41]

TABLE VI
Volume Fraction of Polymer (V_p), Crosslink Density (ν), and Molecular Weight Between Two Crosslinks ($\overline{M}_c$) for the Cationic and Thermal Polymers at 25°C

Sample ID	V_p	$\nu \times 10^6$ (mol/cm^3)	$\overline{M}_c \times 10^{-8}$ (cm^3/mol)
Lin30	0.89393	37.44	1.33547
Lin40	0.87237	31.96	1.564456
Lin50	0.85746	28.82	1.734906
Lin60	0.82823	23.76	2.104377
DCP5	0.8021	20.16	2.480159
DCP7	0.88221	34.30	1.457726
DCP16	0.97918	92.34	0.541477
CLin0	0.975123	86.01	0.581328
CLin10	0.92182	46.97	1.064509
CLin20	0.89976	39.16	1.276813
CLin30	0.87231	31.94	1.565435
CLin40	0.86377	30.09	1.661682
CLin50	0.84169	25.93	1.928268
CLin60	0.80574	20.62	2.42483

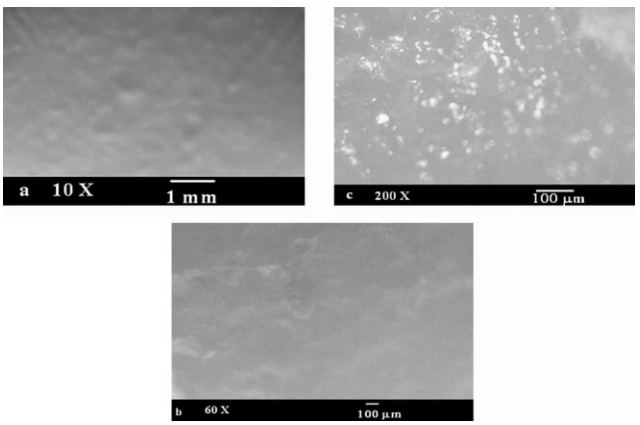

Figure 11 Micrographs of the swelling of the cationic sample containing conjugated linseed oil 50%, acrylic acid 40%, and divinylbenzene 10% (sample CLin50).

$$V_p = \frac{\text{Weight of polymer} \Big/ \text{Density of polymer}}{\text{Weight of polymer} \Big/ \text{Density of polymer} + \text{Weight of solvent} \Big/ \text{Density of solvent}} \tag{8}$$

$$\chi = \chi_H + \chi_S = \frac{V_1(\delta_p - \delta_s)^2}{RT} + 0.34 \tag{9}$$

Where χ_H and χ_S are the enthalpic and entropic components of χ, δ_p and δ_s are the solubility parameters of polymers and solvent, respectively. The solubility parameter of the polymer is obtained by fitting the swelling coefficients of the polymer in various solvents. The results are reported in Table VI. The molecular weight between two crosslinks ($\overline{M}_c$) is also calculated for all the samples by following equation[34]

$$\overline{M}c = \frac{1}{2\nu} \tag{10}$$

The values of the crosslink density and $\overline{M}_c$ are reported in Table VI. The crosslink density for cationic samples is the highest for DCP16 and the lowest for DCP5 samples. It is observed that the crosslink density increases with an increase in crosslinker contents, namely, DVB and DCP. That is the reason for showing a maximum and a minimum solvent uptake for DCP5 and DCP 16 samples, respectively. DCP16 sample shows maximum diffusion coefficient, which indicates that the sample present a maximum resistance to the solvent molecules. The crosslink density shows a decrease with an increase in the oil contents.

In thermal samples, CLin0 shows a maximum and CLin60 shows a minimum crosslink density. It is observed that the crosslink density decreases with an increase in oil contents. The decrease in crosslink density increases the solvent uptake. This explains the solvent uptake trends for the thermal polymers.

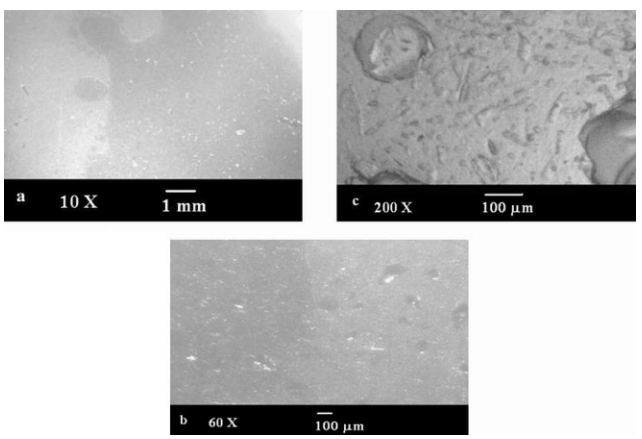

Figure 10 Micrographs of the swelling of the cationic sample containing linseed oil 50%, styrene 30%, and divinylbenzene 20% (sample Lin50).

Optical micrographs of the samples

Figures 10 and 11 show the micrographs of the polymer samples immediately after the completion of the

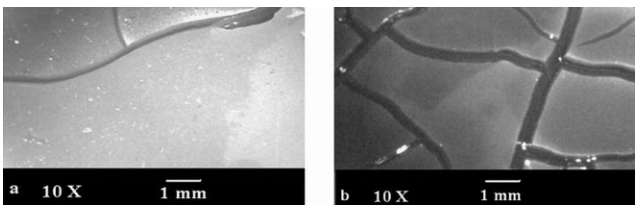

Figure 12 Crack propagation in the samples during escape of solvent after swelling (a) after 10 min and (b) after 40 min.

sorption experiments. In Figure 10, trapped solvent can be observed in the polymer matrix for cationic sample (Lin50). Figure 10(a) is at a magnification of 10 times at 1 mm scale and the solvent can be observed in the polymer matrix in the form of dark areas. In Figure 10(b), the escaping droplets are apparent and in Figure 10(c), some pore can be seen on the matrix with the marks of solvent evaporation from the sample. In Figure 11(a,b), smooth surface is observed for thermal sample (CLin50) and at a higher magnification (200×) in Figure 11(c), shining gel-like appearance can clearly be observed. This is the clear indication that the thermal polymer has resisted the solvent, and therefore swelling is less than the cationic samples. When the sample is observed for about 30 min under microscope, the cracks on the surface of polymer are observed. These cracks are the result of the internal stresses of the solvent molecules, which try to escape from the matrix. The propagation of cracks in the polymer matrix is shown in Figure 12. When sample is removed from solvent, few cracks developed on the surface of the polymer sample after 10 min [Fig. 12(a)]. The cracks keep on increasing with the escape of the solvent from the polymer [Fig. 12(b)].

CONCLUSIONS

A new system of linseed oil-based polymers is investigated for the sorption and diffusion studies. The kinetics of the sorption is studied by using the equation of transport phenomena. The values of n in transport equation are found to be below 0.4, showing the non-Fickian diffusion in the polymer. The dependence of the diffusion coefficient on the composition and temperature has been studied for the polymeric samples. The diffusion coefficient in cationic samples decreases with an increase in the oil contents in the samples, and in thermal samples, it first increases up to 30% oil contents and then decreases. The diffusion coefficient decreases with an increase in temperature for all polymer samples. The sorption coefficient increases with an increase in the oil contents for all samples. The crosslink density and the molecular weight between two crosslinks show a decrease with an increase in the oil contents in both cationic and thermal polymers. The crosslink density ranges from 20.16 to 92.34 $\times$ 10^6 mol/cm^3 for cationic samples and 20.62 to 86.01 $\times$ 10^6 mol/cm^3 for thermal samples.

References

1. Gouanve, F.; Marais, S.; Bessadok, A.; Langevin, D.; Metayer, M. Eur Polym J 2007, 43, 586.
2. Hansen, C. M. Prog Org Coat 2004, 51, 55.
3. Tanigami, T.; Yano, K.; Yamaura, K.; Matsuzawa, S. Polymer 1995, 36, 2941.
4. Zhu, Q.; Shentu, B.; Liu, Q.; Weng, Z. Eur Polym J 2006, 42, 1417.
5. Detallante, V.; Langevin, D.; Chappey, C.; Metayer, M.; Mercier, R.; Pineri, M. Desalination 2002, 148, 333.
6. Kumar, R.; Srivastava, S. K.; Mathur, G. N. J Elast Plast 1985, 17, 89.
7. Han, H.; Gryte, C. C.; Ree, M. Polymer 1995, 36, 1663.
8. Singh, P.; Kaushik, A.; Gupta, P. J Reinf Plast Compos 2005, 24, 1479.
9. Sen, M.; Guven, O. Comput Theor Polym Sci 2000, 11, 475.
10. Singh, P. P.; Cushman, J. H.; Maier, D. E. Chem Eng Sci 2003, 58, 2409.
11. Altinkaya, S. A.; Ramesh, N.; Duda, J. L. Polymer 2006, 47, 8228.
12. Fieldson, G. T.; Barbari, T. A. Polymer 1993, 34, 1146.
13. Philippe, L.; Sammon, C.; Lyon, S. B.; Yarwood, J. Prog Org Coat 2004, 49, 302.
14. Philippe, L.; Sammon, C.; Lyon, S. B.; Yarwood, J. Prog Org Coat 2004, 49, 315.
15. Conte, L. S.; Lercker, G.; Capella, P.; Catena, M. Rivista Italiana delle Sostanze Grasse 1979, 56, 339.
16. Berglund, D. R. In Trends in New Crops and New Uses; Janick, J., Whipkey, A., Eds.; ASHS Press: Alexandria, 2002; p 358.
17. Knorr, W.; Daute, P.; Grutzmacher, R.; Hofer, R. Fat Sci Technol 1995, 97, 165.
18. Budwig, J. Flax Oil as a True Aid Against Arthritis, Heart Infarction, Cancer and Other Diseases; Apple Publication: Vancouver, 1996.
19. Motawie, A. M.; Hassan, F. A.; Manieh, A. A.; Aboul-Fetouh, M. E.; El-Din, A. F. J. J Appl Polym Sci 1995, 55, 1725.
20. Thames, S. F.; Hariharan, R.; Wang, Z.; Brister, E. H.; King, C. L.; Panjanani, K. G. U.S. Pat. 6,624,223 (2003).
21. Tortorello, A. J.; Montgomery, E.; Chawla, C. P. U.S. Pat. 6,638,616 (2003).
22. Gultekin, M.; Beker, U.; Güner, F. S.; Erciyes, A. T.; Yagci, Y. Macromol Mater Eng 2000, 283, 15.
23. Ajithkumar, S.; Patel, N. K.; Kansara, S. S. Polym Gels Networks 1998, 6, 137.
24. Bagley, E.; Long, F. A. J Am Chem Soc 1955, 77, 2172.
25. Zeng, C.; Li, J.; Li, P.; Chen, T.; Lin, Y.; Wang, D.; Chen, C. Chem Eng Sci 2006, 61, 1892.
26. Neff, W. E.; Frankel, E. N.; Pryde, E. H.; Riser, G. R. J Am Oil Chem Soc 1976, 53, 152.
27. Nandanan, V.; Joseph, R.; Francis, D. J. J Elast Plast 1996, 28, 326.
28. Benecke, H. P.; Vijayendran, B. R.; Elhard, J. D. U.S. Pat. 6,797,753 (2004).
29. George, S. C.; Knorgen, M.; Thomas, S. J Membr Sci 1999, 163, 1.

30. Crank, J. The Mathematics of Diffusion, 2nd ed.; Clarendon Press: Oxford, 1975; Chapter 11.
31. Rogers, C. E. In Polymer Permeability, 1st ed.; Comyn, J., Eds.; Chapman and Hall: U.K., 1985; p 11.
32. Windle, A. H. In Polymer Permeability, 1st ed.; Comyn, J., Eds.; Chapman and Hall: U.K., 1985; p 75.
33. Ajithkumar, S.; Patel, N. K.; Kansara, S. S. Eur Polym J 2000, 36, 2387.
34. Mathew, A. P.; Packirisamy, S.; Kumaran, M. G.; Thomas, S. Polymer 1995, 36, 4935.
35. Meares, P. J Am Chem Soc 1954, 76, 3415.
36. Galiatsatou, P.; Kanellopoulos, N. K.; Petropoulos, J. H. J Membr Sci 2006, 280, 634.
37. Hayashi, Y.; Sugiyama, S.; Kawanishi, T.; Shimizu, N. J Membr Sci 1999, 156, 11.
38. Islam, M. A.; Buschatz, H. Chem Eng Sci 2002, 57, 2089.
39. Mcdowell, C. C.; Freeman, B. D.; Mcneely, G. W. Polymer 1999, 40, 3487.
40. Hu, D. S. G.; Chou, K. J. N. Polymer 1996, 37, 1019.
41. Zhu, L.; Wool, R. P. Polymer 2006, 47, 8106.